

A novel nonlinear vibration feature-based approach for evaluating bolt-loosening faults in aerospace structures

Quankun Li¹ and Xingjian Jing²

¹ School of Power and Energy, Northwestern Polytechnical University, People's Republic of China

² Department of Mechanical Engineering, City University of Hong Kong, Hong Kong, People's Republic of China

ABSTRACT

Aerospace structures such as aircraft and satellites are frequently subjected to bolt-loosening faults in service, which will seriously affect structural integrity, reliability and safety. In this paper, the development of a novel approach based on nonlinear vibration features is presented to evaluate potential bolt-loosening faults in these structures. Firstly, the complex aerospace structure is decomposed into some simple T-type substructures based on structural configurations and features. Then, a general T-type multi-degree-of-freedom (MDOF) model simulating bolt-loosening faults and nonlinear boundaries as nonlinear damper-spring components is built for nonlinear vibration analysis. After that, two novel fault features, which are functions of structural properties, nonlinear output spectra and bolt-loosening fault-induced forces, are defined to form a novel bolt-loosening fault indicator. Finally, a novel approach with detailed operational procedures is proposed, and its effectiveness and superiority are verified through experimental studies on a simple lab structure with bolt-loosening faults and nonlinear boundaries.

KEYWORDS Aerospace structure; bolt-loosening fault; nonlinear vibration; transmissibility function; fault evaluation

CONTACT Quankun Li ✉ quankun_li@hotmail.com

Received 26 February 2023

1. Introduction

In aerospace structures including aircraft, satellites, rockets and engines, bolt joints are frequently applied to assemble different components together. However, since these structures usually encounter various dynamic operational loads like vibration and shock in service, bolt joints inevitably undergo slip, collision and rubbing, which in turn lead to bolt-loosening faults, and may cause structural failure or cause catastrophic accidents (Bickford, 2008; Bickford and Nassar, 1998). Thus, it is meaningful and essential to evaluate bolt-loosening faults as early as possible in terms of economics and safety (Balageas et al., 2010).

Considering the nonlinear effects of bolt-loosening faults on structures, plenty of evaluation approaches based on nonlinear vibration features have been proposed (Miao et al., 2020; Nikraves and Goudarzi, 2017). In these approaches, healthy structures without faults are linear systems and damaged structures with bolt-loosening faults are nonlinear systems. Therefore, the existence of nonlinearities in damaged structures can be applied to evaluate bolt-loosening faults (Huang et al., 2022). Commonly applied nonlinear vibration features are natural frequencies, mode shapes, frequency response functions and transmissibility functions. Compared to others, the transmissibility function, generally defined as the ratio of two output spectra, is more sensitive to the existence of bolt-loosening faults and has simpler data processing (Li et al., 2021). For example, the identification of natural frequencies and mode shapes requires complex

modal analysis, and the calculation of frequency response functions requires both inputs and outputs.

Johnson and Adams firstly applied properties of nonlinear transmissibility functions for the evaluation of loose bolts in an aircraft panels (2002). Then, a similar fault indicator was applied for the damage prognosis in rotorcraft fuselage with bolt-loosening faults (Brown and Adams, 2003). After that, an advanced logarithm was utilised to normalise nonlinear transmissibility functions, and an improved bolt-loosening fault indicator named transmissibility function power was proposed (Johnson et al., 2004). To reduce the influence of excitation and increase the weight of resonance, a weighting factor was used to amplify the difference between the transmissibility functions of structures before and after bolt-loosening faults (Li et al., 2015). Apart from output spectra, a coherence function was applied to define the transmissibility functions as well, and a bolt-loosening fault indicator was defined by the modal assurance criterion (MAC) (Zhou et al., 2015). To consider high-frequency band features, wavelet transform was applied to process data, and the properties of wavelet-based transmissibility functions were applied for bolt-loosening faults in a one-dimensional multi-degree-of-freedom (MDOF) system (Li et al., 2017).

Since aerospace structures with bolt-loosening faults are typical nonlinear systems, the relation between inputs and outputs can be described by the Volterra series as well (Jing and Li, 2016). Based on this, a nonlinear output frequency response function (NOFRF) was applied to define transmissibility functions, and a related fault indicator was applied for detecting potential bolt-loosening

faults in a two-dimensional structure (Cheng et al., 2014). Similar to this, an improved method using sinusoidal inputs was developed to calculate NOFRFs and the corresponding fault indicator (Peng et al., 2010). According to the relations between nonlinear output spectra and NOFRFs, a new nonlinear transmissibility function-based approach was proposed to evaluate the number and position of bolt-loosening faults in frame structures (Zhao et al., 2014). With the merit of the second-order output spectrum (SOOS) which is more sensitive to initial and tiny faults, a novel approach using SOOS transmissibility functions was applied to evaluate loose bolts in a satellite structure (Li and Jing, 2017). Later, an improved method, eliminating the effects of inherent material nonlinearities, was proposed for bolt loosening faults in the same satellite structure (Li and Jing, 2020a). Considering the bolt-loosening faults with different severities in the satellite structure, a new approach encompassing the local tuning approach (LTA) and SOOS transmissibility functions was proposed for diagnosis (Li and Jing, 2020b). Recently, a novel frequency domain feature-based approach for diagnosing bolt-loosening faults in complex structures without reference data was proposed and verified (Li and Jing, 2022).

Although the effectiveness of the above approaches based on nonlinear transmissibility functions have been verified through experiments, some limitations should be considered to improve them: (1) Most methods are more applicable to simple beams rather than complex aerospace structures; (2) Nonlinear boundaries, which will be coupled with faults, are ignored in most approaches; (3) Most methods require the entire model and responses of structures, inevitably thereby increasing the practical operating complexities.

To consider the above limitations, a novel approach for evaluating potential bolt-loosening faults in aerospace structures using nonlinear transmissibility functions is proposed in this paper. Significant novelties and contributions of this paper are: (1) Complex aerospace structures are decomposed into some simple T-type substructures based on the structural characteristics; (2) In the T-type MDOF model, both bolt-loosening faults and nonlinear boundaries are simulated as nonlinear connecting elements; (3) With two fault features, obtained from the substructure to be evaluated only, a novel indicator is obtained, and its effectiveness is verified through comparison studies on a lab bolted structure.

Besides the first section, this paper has four main sections. Some dynamic features of T-type substructures in complex aerospace structures are analysed in section 2. The fundamentals of the novel approach including features, indicator and procedures are shown in section 3. Experimental studies are completed in section 4, and conclusions and discussions of this paper are summarised in section 5.

2. Aerospace structures and the T-type MDOF model

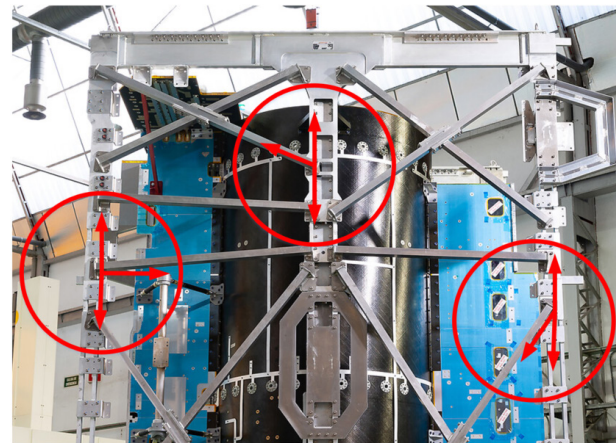


Figure 1. Substructures in a bolted satellite structure.

Figure 1 shows that complex aerospace structures (taking a bolted satellite structure as an example) can be decomposed into a series of very simple T-type substructures based on vibration paths and structural configurations. Thus, the nonlinear dynamic behaviour of complex structures can be described by analysing these substructures in sequence. Referring to the general discrete MDOF model applied for simple beams, the T-type MDOF model of substructures can be obtained accordingly, which includes some simple mass-damper-spring elements (Cheng and Cigada, 2020).

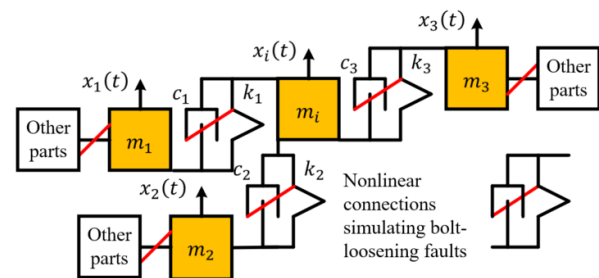


Figure 2. The T-type MDOF model.

As shown in Figure 2, three adjacent masses are connected to the central mass with damper-spring connections in the T-type MDOF model. Nonlinear boundaries and excitations exist at other structural parts. Since bolt-loosening faults and nonlinear boundaries usually affect structural damping and stiffness properties only, they are generally simulated as nonlinear connections in the T-type MDOF model (Johnson and Adams, 2002).

Considering the vertical motion of all masses in the T-type Model, the differential equation of motion of central mass m_i can be formulated based on Newton's second law (Ewins, 2000), as

$$\begin{aligned}
 & m_i x_i''(t) + c_1(x_i'(t) - x_1'(t)) + k_1(x_i(t) - x_1(t)) \\
 & + c_2(x_i'(t) - x_2'(t)) + k_2(x_i(t) - x_2(t)) \\
 & + c_3(x_i'(t) - x_3'(t)) + k_3(x_i(t) - x_3(t)) = s_i^{faul}(t)
 \end{aligned} \quad (1)$$

where m_i , c_1 , c_2 , c_3 , k_1 , k_2 and k_3 are structural mass, damping and stiffness coefficients respectively. $x_i''(t)$ is the acceleration of mass m_i , $x_i'(t)$, $x_1'(t)$, $x_2'(t)$ and $x_3'(t)$ are velocities of mass m_i , and $x_i(t)$, $x_1(t)$, $x_2(t)$ and $x_3(t)$ are displacements of mass m_i . $s_i^{faul}(t)$ represents the bolt-loosening fault-induced force applied to mass m_i .

Potential bolt-loosening faults can cause changes not only in linear structural properties but also nonlinear behaviours of substructures. Thus, their effects are generally described as nonlinear fault-induced forces, which are functions of velocities and displacements (Johnson and Adams, 2002).

$$\begin{aligned}
 & s_i^{faul}(t) \\
 & = \sum_{p=1}^{\infty} \begin{pmatrix} -c_{1,p}(x_i'(t) - x_1'(t))^p - k_{1,p}(x_i(t) - x_1(t))^p \\ -c_{2,p}(x_i'(t) - x_2'(t))^p - k_{2,p}(x_i(t) - x_2(t))^p \\ -c_{3,p}(x_i'(t) - x_3'(t))^p - k_{3,p}(x_i(t) - x_3(t))^p \end{pmatrix},
 \end{aligned} \quad (2)$$

where subscript p represents the order of polynomial function, and parameters $c_{1,p}$, $c_{2,p}$, $c_{3,p}$, $k_{1,p}$, $k_{2,p}$ and $k_{3,p}$ are connecting coefficients caused by faults.

On the whole, considering T-type substructures in complex aerospace structures and simulating the effects of faults as equivalent nonlinear forces, the T-type MDOF model and related dynamic equation can be obtained for the dynamic analysis and fault evaluation.

3. A novel fault evaluation approach

3.1. Transmissibility function

If the excitation applied to the aerospace structure is a harmonic function with amplitude, frequency and phase, responses of masses in the T-type model can be obtained based on the harmonic balance method (HBM) (Liu et al., 2006), as

$$z_o(t) = \sum_{v=-\infty}^{\infty} Z_o^{v,A}(jv\omega) e^{jv\omega t}, (o = i, 1, 2, 3), \quad (3)$$

where superscript v means the harmonic order, and $Z_o^{v,A}(jv\omega) e^{jv\omega t}$ is the v^{th} order output spectrum.

Substituting output responses Equation (3) into (1), and equating coefficients of $e^{jv\omega t}$ yields

$$\begin{aligned}
 & \begin{pmatrix} -v\omega^2 m_i + jv\omega c_1 + k_1 \\ +jv\omega c_2 + k_2 + jv\omega c_3 + k_3 \end{pmatrix} Z_i^{v,A}(jv\omega) \\
 & - (jv\omega c_1 + k_1) Z_1^{v,A}(jv\omega) \\
 & - (jv\omega c_2 + k_2) Z_2^{v,A}(jv\omega) \\
 & - (jv\omega c_3 + k_3) Z_3^{v,A}(jv\omega) = S_i^{faul}(jv\omega)
 \end{aligned} \quad (4)$$

where $Z_i^{v,A}(jv\omega)$, $Z_1^{v,A}(jv\omega)$, $Z_2^{v,A}(jv\omega)$ and $Z_3^{v,A}(jv\omega)$ are output spectra of masses, and $S_i^{faul}(jv\omega)$ is the frequency domain bolt-loosening fault-induced force applied to mass m_i .

With output spectra in Equation (4), nonlinear transmissibility functions of the T-type model in Figure 2 can be defined, as

$$\begin{aligned}
 & T_{a,b}^{v,A}(jv\omega) = \frac{Z_a^{v,A}(jv\omega)}{Z_b^{v,A}(jv\omega)}, \\
 & (a, b = i, 1, 2, 3, a \neq b, v \geq 1)
 \end{aligned} \quad (5)$$

where $Z_a^{v,A}(jv\omega)$ and $Z_b^{v,A}(jv\omega)$ are the output spectra of two arbitrary masses m_a and m_b in the T-type MDOF model respectively.

3.2. Fault features and indicator

With nonlinear transmissibility functions defined in Equation (5), two novel fault features and one indicator are derived in this section.

Rewriting Equation (4) gives

$$\begin{aligned}
 & \begin{pmatrix} -v\omega^2 m_i + jv\omega c_1 + k_1 \\ +jv\omega c_2 + k_2 + jv\omega c_3 + k_3 \end{pmatrix} \\
 & - (jv\omega c_1 + k_1) \frac{Z_1^{v,A}(jv\omega)}{Z_i^{v,A}(jv\omega)} \\
 & - (jv\omega c_2 + k_2) \frac{Z_2^{v,A}(jv\omega)}{Z_i^{v,A}(jv\omega)} \\
 & - (jv\omega c_3 + k_3) \frac{Z_3^{v,A}(jv\omega)}{Z_i^{v,A}(jv\omega)} = \frac{S_i^{faul}(jv\omega)}{Z_i^{v,A}(jv\omega)}
 \end{aligned} \quad (6)$$

With Equation (5), Equation (6) becomes

$$\begin{aligned}
 & \begin{pmatrix} -v\omega^2 m_i + jv\omega c_1 + k_1 \\ +jv\omega c_2 + k_2 + jv\omega c_3 + k_3 \end{pmatrix} \\
 & - (jv\omega c_1 + k_1) T_1^{v,A}(jv\omega) \\
 & - (jv\omega c_2 + k_2) T_2^{v,A}(jv\omega) \\
 & - (jv\omega c_3 + k_3) T_3^{v,A}(jv\omega) = \frac{S_i^{faul}(jv\omega)}{Z_i^{v,A}(jv\omega)}
 \end{aligned} \quad (7)$$

Now, exciting the structure four times with different excitation magnitudes, four equations similar to Equation (7) can be obtained, as

$$\begin{aligned}
 &(-v\omega^2 m_i + jv\omega c_1 + k_1 + jv\omega c_2 + k_2 + jv\omega c_3 + k_3) \\
 &-(jv\omega c_1 + k_1)T_1^{v,A^r}(jv\omega) - (jv\omega c_2 + k_2)T_2^{v,A^r}(jv\omega) \quad (8) \\
 &-(jv\omega c_3 + k_3)T_3^{v,A^r}(jv\omega) = \frac{S_i^{fa,u,A^r}(jv\omega)}{Z_i^{v,A^r}(jv\omega)}, (r=1,2,3,4)
 \end{aligned}$$

Using any three of the equations in (8) and rewriting them in a matrix form gives

$$\begin{aligned}
 &[T^u(jv\omega)]_{\substack{3 \times 3 \\ 3 \times 1}} [A(jv\omega)]_{\substack{3 \times 1 \\ 3 \times 1}} \\
 &= [B(jv\omega)]_{\substack{3 \times 3 \\ 3 \times 1}} + [C^u(jv\omega)]_{\substack{3 \times 1 \\ 3 \times 1}}, (u=1,2) \quad (9)
 \end{aligned}$$

where

$$[T^1(jv\omega)] = \begin{bmatrix} T_1^{v,A^1}(jv\omega) & T_2^{v,A^1}(jv\omega) & T_3^{v,A^1}(jv\omega) \\ T_1^{v,A^2}(jv\omega) & T_2^{v,A^2}(jv\omega) & T_3^{v,A^2}(jv\omega) \\ T_1^{v,A^3}(jv\omega) & T_2^{v,A^3}(jv\omega) & T_3^{v,A^3}(jv\omega) \end{bmatrix}, \quad (10a)$$

$$[T^2(jv\omega)] = \begin{bmatrix} T_1^{v,A^2}(jv\omega) & T_2^{v,A^2}(jv\omega) & T_3^{v,A^2}(jv\omega) \\ T_1^{v,A^3}(jv\omega) & T_2^{v,A^3}(jv\omega) & T_3^{v,A^3}(jv\omega) \\ T_1^{v,A^4}(jv\omega) & T_2^{v,A^4}(jv\omega) & T_3^{v,A^4}(jv\omega) \end{bmatrix}, \quad (10b)$$

$$[A(jv\omega)] = \begin{bmatrix} jv\omega c_1 + k_1 \\ jv\omega c_2 + k_2 \\ jv\omega c_3 + k_3 \end{bmatrix}, \quad (10c)$$

$$[B(jv\omega)] = \begin{bmatrix} -v\omega^2 m_0 + jv\omega c_1 + k_1 \\ +jv\omega c_2 + k_2 + jv\omega c_3 + k_3 \\ -v\omega^2 m_0 + jv\omega c_1 + k_1 \\ +jv\omega c_2 + k_2 + jv\omega c_3 + k_3 \\ -v\omega^2 m_0 + jv\omega c_1 + k_1 \\ +jv\omega c_2 + k_2 + jv\omega c_3 + k_3 \end{bmatrix}, \quad (10d)$$

$$[C^1(jv\omega)] = \begin{bmatrix} \frac{S_i^{fa,u,A^1}(jv\omega)}{Z_i^{v,A^1}(jv\omega)} \\ \frac{S_i^{fa,u,A^2}(jv\omega)}{Z_i^{v,A^2}(jv\omega)} \\ \frac{S_i^{fa,u,A^3}(jv\omega)}{Z_i^{v,A^3}(jv\omega)} \\ \frac{S_i^{fa,u,A^4}(jv\omega)}{Z_i^{v,A^4}(jv\omega)} \end{bmatrix} [C^2(jv\omega)] = \begin{bmatrix} \frac{S_i^{fa,u,A^2}(jv\omega)}{Z_i^{v,A^2}(jv\omega)} \\ \frac{S_i^{fa,u,A^3}(jv\omega)}{Z_i^{v,A^3}(jv\omega)} \\ \frac{S_i^{fa,u,A^4}(jv\omega)}{Z_i^{v,A^4}(jv\omega)} \end{bmatrix}. \quad (10e)$$

With the inverse matrix $[D^u(jv\omega)] = [T^u(jv\omega)]^{-1}$, Equation (9) becomes

$$\begin{aligned}
 &[A(jv\omega)]_{\substack{3 \times 1 \\ 3 \times 1}} = [D^u(jv\omega)]_{\substack{3 \times 3 \\ 3 \times 3}} [B(jv\omega)]_{\substack{3 \times 1 \\ 3 \times 1}} \\
 &+ [D^u(jv\omega)]_{\substack{3 \times 3 \\ 3 \times 3}} [C^u(jv\omega)]_{\substack{3 \times 1 \\ 3 \times 1}}, (u=1,2) \quad (11)
 \end{aligned}$$

Through Equation (11), the last two elements in matrix $[A(jv\omega)]$ can be calculated respectively, as

$$\begin{aligned}
 &jv\omega c_2 + k_2 = D_{2,1}^1(jv\omega)B_{1,1}(jv\omega) \\
 &+ D_{2,2}^1(jv\omega)B_{2,1}(jv\omega) + D_{2,3}^1(jv\omega)B_{3,1}(jv\omega), \\
 &+ D_{2,1}^1(jv\omega)C_{1,1}^1(jv\omega) \\
 &+ D_{2,2}^1(jv\omega)C_{2,1}^1(jv\omega) + D_{2,3}^1(jv\omega)C_{3,1}^1(jv\omega) \quad (12a)
 \end{aligned}$$

$$\begin{aligned}
 &jv\omega c_3 + k_3 = D_{3,1}^1(jv\omega)B_{1,1}(jv\omega) \\
 &+ D_{3,2}^1(jv\omega)B_{2,1}(jv\omega) + D_{3,3}^1(jv\omega)B_{3,1}(jv\omega), \\
 &+ D_{3,1}^1(jv\omega)C_{1,1}^1(jv\omega) \\
 &+ D_{3,2}^1(jv\omega)C_{2,1}^1(jv\omega) + D_{3,3}^1(jv\omega)C_{3,1}^1(jv\omega) \quad (12b)
 \end{aligned}$$

$$\begin{aligned}
 &jv\omega c_2 + k_2 = D_{2,1}^2(jv\omega)B_{1,1}(jv\omega) \\
 &+ D_{2,2}^2(jv\omega)B_{2,1}(jv\omega) + D_{2,3}^2(jv\omega)B_{3,1}(jv\omega), \\
 &+ D_{2,1}^2(jv\omega)C_{1,1}^2(jv\omega) \\
 &+ D_{2,2}^2(jv\omega)C_{2,1}^2(jv\omega) + D_{2,3}^2(jv\omega)C_{3,1}^2(jv\omega) \quad (12c)
 \end{aligned}$$

$$\begin{aligned}
 &jv\omega c_3 + k_3 = D_{3,1}^2(jv\omega)B_{1,1}(jv\omega) \\
 &+ D_{3,2}^2(jv\omega)B_{2,1}(jv\omega) + D_{3,3}^2(jv\omega)B_{3,1}(jv\omega), \\
 &+ D_{3,1}^2(jv\omega)C_{1,1}^2(jv\omega) \\
 &+ D_{3,2}^2(jv\omega)C_{2,1}^2(jv\omega) + D_{3,3}^2(jv\omega)C_{3,1}^2(jv\omega) \quad (12d)
 \end{aligned}$$

With Equation (12), two novel fault features can be defined, as

$$\begin{aligned}
 \eta_1^1(jv\omega) &= \frac{jv\omega c_2 + k_2 - D_{2,1}^1(jv\omega)C_{1,1}^1(jv\omega)}{jv\omega c_3 + k_3 - D_{3,1}^1(jv\omega)C_{1,1}^1(jv\omega)} \\
 &- \frac{D_{2,2}^1(jv\omega)C_{1,1}^1(jv\omega) - D_{2,3}^1(jv\omega)C_{1,1}^1(jv\omega)}{D_{3,2}^1(jv\omega)C_{1,1}^1(jv\omega) - D_{3,3}^1(jv\omega)C_{1,1}^1(jv\omega)}, \\
 &= \frac{D_{2,1}^1(jv\omega) + D_{2,2}^1(jv\omega) + D_{2,3}^1(jv\omega)}{D_{3,1}^1(jv\omega) + D_{3,2}^1(jv\omega) + D_{3,3}^1(jv\omega)} \quad (13a)
 \end{aligned}$$

$$\begin{aligned}
 \eta_1^2(jv\omega) &= \frac{jv\omega c_2 + k_2 - D_{2,1}^2(jv\omega)C_{1,1}^2(jv\omega)}{jv\omega c_3 + k_3 - D_{3,1}^2(jv\omega)C_{1,1}^2(jv\omega)} \\
 &- \frac{D_{2,2}^2(jv\omega)C_{1,1}^2(jv\omega) - D_{2,3}^2(jv\omega)C_{1,1}^2(jv\omega)}{D_{3,2}^2(jv\omega)C_{1,1}^2(jv\omega) - D_{3,3}^2(jv\omega)C_{1,1}^2(jv\omega)}, \\
 &= \frac{D_{2,1}^2(jv\omega) + D_{2,2}^2(jv\omega) + D_{2,3}^2(jv\omega)}{D_{3,1}^2(jv\omega) + D_{3,2}^2(jv\omega) + D_{3,3}^2(jv\omega)} \quad (13b)
 \end{aligned}$$

From Equation (13), it is shown that if there is no fault around mass m_i in the T-type model (Figure 2), potential bolt-loosening fault-induced force $S_i^{fa,u,A^r}(jv\omega)$ ($r=1,2,3,4$) applied to mass m_i will be zero. And then, two fault features have the same expression and value. On the contrary, if there is a fault around mass m_i , potential bolt-loosening fault-induced force $S_i^{fa,u,A^r}(jv\omega)$ ($r=1,2,3,4$) applied to mass m_i will be nonzero, which in turn leads to different and nonequal fault features. On the other hand, fault features can be directly calculated by nonlinear transmissibility functions in matrix $[T^u(jv\omega)]$.

Therefore, with the properties of novel fault features in Equation (13), a local fault indicator can be defined as the relative change between two fault features, whose value, zero or nonzero, can be used to evaluate whether there is a bolt-loosening fault in the T-type substructure (Figure 2).

$$\psi_i(j\omega) = \left| \frac{\sum_{v=1}^V \eta_i^1(jv\omega) - \sum_{v=1}^V \eta_i^2(jv\omega)}{\sum_{v=1}^V \eta_i^1(jv\omega)} \right| * 100, \quad (14)$$

where V is the maximum harmonic order.

3.3. Procedures and remarks

With the derivation of fault features and fault indicator, a novel bolt-loosening fault evaluation approach can be proposed.

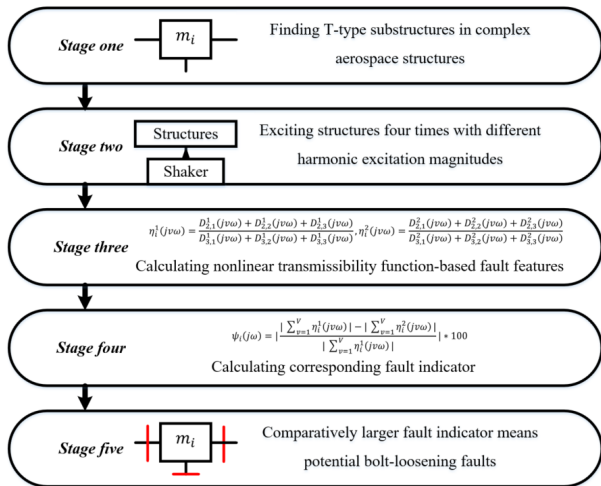


Figure 3. Procedures of the approach.

Figure 3 shows that this novel approach has five main stages. Firstly, the condition of the aerospace structure is checked and related T-type substructures to be evaluated are found. Then, the structure is excited four times with different excitation magnitudes and signals of substructures are processed with MATLAB codes. With output spectra, fault features and related fault indicators are computed with Equation (13) and (14) respectively. Finally, whether there is a bolt-loosening fault or not in each substructure is determined according to the value of related indicators.

Compared with existing fault evaluation approaches with nonlinear transmissibility functions, this novel proposed approach considering local T-type substructures to be evaluated only has obvious features. For example, it does not require an entire model and whole responses of complex aerospace structures. It eliminates the coupling effects of nonlinear boundaries. It does not need reference data of healthy structures as well. Therefore, this new approach will be much more effective and convenient in practical application.

4. Experimental verification

To verify the effectiveness of the proposed approach, some tests on a lab bolted structure are performed.

4.1. Experimental setup

The bolted structure, which is used to simulate bolted frames in aerospace structures is connected by some steel bars and bolted joints (Figure 4). Four masses ($m1$, $m5$,

$m11$ and $m15$) at corners are connected to the fixed ground to represent nonlinear boundaries, and the mass $m15$ is attached to the shaker. Bolts in two T-type substructures marked by blue and green colours are to be evaluated.

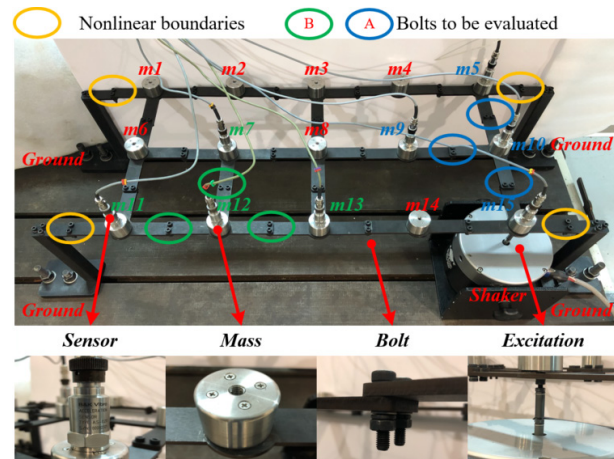


Figure 4. The bolted structure.

As shown in Table 1, two cases are to be studied. For the healthy structure, all bolts are initially fastened with 4 Nm torque (tightened state). In case one, only one bolt in substructure A is loosened to simulate the single fault. In case two, both substructures have loose bolts to simulate multiple faults. Nonlinear boundaries exist in the healthy structure as well as the damaged structure.

Table 1. Details of cases.

Structure		Conditions
Healthy structure		Bolts are in a tightened state
Damaged structure	Case one	One fault is between masses $m9$ and $m10$ in substructure A.
	Case two	One fault is between masses $m9$ and $m10$ in substructure A, and one fault is between masses $m7$ and $m12$ in substructure B.

Excitations generated by the RIGOL function generator (RIGOL.com, 2023) are transmitted to the B&K shaker (B&K.com, 2023a), and then, vertical vibration data are acquired by B&K Vibro-sensors (B&K.com, 2023b) installed on related masses. Technical specifications of all data acquisition devices are shown in Table 2.

Table 2. Details of devices.

Device	Item	Value
RIGOL function generator	Sample rate	500MSa/s
	Maximum frequency	100MHz
B&K shaker	Frequency range	DC-5000Hz
	Rated force	100N
B&K Vibro-sensors	Measuring range	±40g
	Sensitivity	100mv/g

Table 3. Results of the novel approach.

Case	Term	Mass block	
		10	12
One	$ \sum_{v=1}^V \eta_i^1(jv\omega) $	5.630	37.939
	$ \sum_{v=1}^V \eta_i^2(jv\omega) $	9.319	36.214
	$\psi_i(j\omega)(\%)$	65.53	4.55
Two	$ \sum_{v=1}^V \eta_i^1(jv\omega) $	14.865	49.203
	$ \sum_{v=1}^V \eta_i^2(jv\omega) $	10.075	65.418
	$\psi_i(j\omega)(\%)$	32.22	32.96

4.2. Results and analysis

Following the procedures of the novel approach in Figure 3, the experimental results of the novel approach are shown in Table 3 and Figure 5.

For case one, the results in Table 3 and Figure 5 show that the indicator $\psi_{10}(j\omega)$ is relatively larger while index $\psi_{12}(j\omega)$ is almost zero, meaning that only substructure A has bolt-loosening faults in this case. For case two, indicators in both substructures have significantly larger values, illustrating that both substructures have bolt-loosening faults in this case. The evaluated results of two cases are consistent with the case setup in Table 1.

4.3. Comparison with an existing approach

To further verify the superiority of this novel approach, one existing approach (Johnson and Adams, 2002) using general nonlinear transmissibility functions is applied for comparison.

In the MDOF structure, if faults are between masses m_p and m_q , and the single excitation is applied to mass m_l , the properties of general nonlinear transmissibility functions can be summarised, as

$$T_{i,i+1}^r(j\omega) = \frac{Z_i^r(j\omega)}{Z_{i+1}^r(j\omega)}, T_{i,i+1}^d(j\omega) = \frac{Z_i^d(j\omega)}{Z_{i+1}^d(j\omega)}$$

$$DI_{i,i+1}(j\omega) = \left| \frac{T_{i,i+1}^d(j\omega) - T_{i,i+1}^r(j\omega)}{T_{i,i+1}^r(j\omega)} \right| \quad (15a)$$

$$\begin{cases} DI_{i,i+1}(j\omega) \neq 0, (1 \leq i < p) \\ DI_{i,i+1}(j\omega) \neq 0, (p \leq i < q) \\ DI_{i,i+1}(j\omega) = 0, (q \leq i < n) \end{cases} \quad (15b)$$

where superscripts r and d represent the quantities obtained from healthy and damaged structures respectively, $Z_i(j\omega)$ and $Z_{i+1}(j\omega)$ are output spectra of masses m_i and m_{i+1} respectively, and $DI_{i,i+1}(j\omega)$ is the fault indicator.

Equation (15) illustrates that nonlinear transmissibility functions of healthy and damaged structures within $(1 \leq i < q)$ are different, which in turn leads to a comparatively larger fault indicator $DI_{i,i+1}(j\omega)$. The results of this approach for two cases are shown in Table 4 and Table 5 respectively.

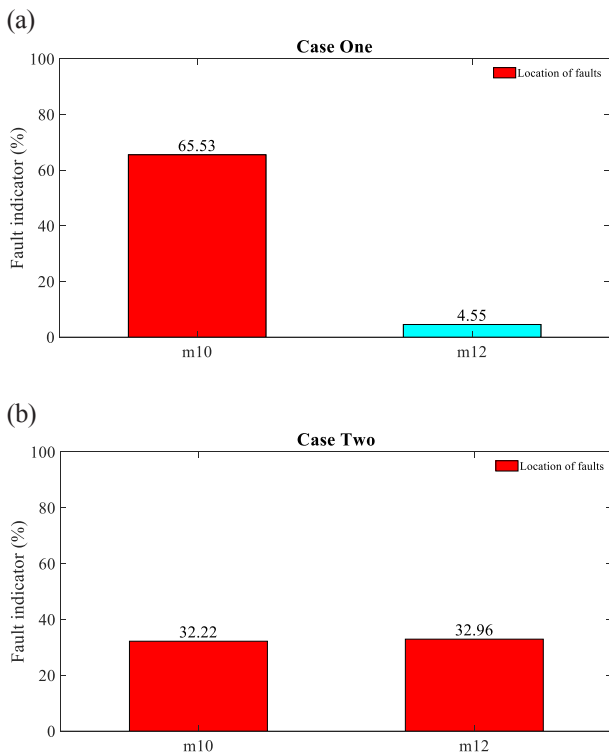


Figure 5. Results of the novel approach.

Table 4. Results of the existing approach for case one.

Experiment	Term	Masses in substructure A		
		05/10	09/10	15/10
Health structure	$T_{i,i+1}^r(j\omega)$	6.533	7.911	8.075
Case one	$T_{i,i+1}^d(j\omega)$	4.909	5.872	6.435
	$DI_{i,i+1}(j\omega)$	0.25	0.26	0.20
Experiment	Term	Masses in substructure B		
		07/12	11/12	13/12
Health structure	$T_{i,i+1}^r(j\omega)$	0.199	0.417	0.580
Case one	$T_{i,i+1}^d(j\omega)$	0.199	0.422	0.557
	$DI_{i,i+1}(j\omega)$	0.00	0.01	0.04

Table 5. Results of the existing approach for case two.

Experiment	Term	Masses in substructure A		
		05/10	09/10	15/10
Health structure	$T_{i,i+1}^r(j\omega)$	6.533	7.911	8.075
Case two	$T_{i,i+1}^d(j\omega)$	4.909	5.857	6.509
	$DI_{i,i+1}(j\omega)$	0.25	0.26	0.19
Experiment	Term	Masses in substructure B		
		07/12	11/12	13/12
Health structure	$T_{i,i+1}^r(j\omega)$	0.199	0.417	0.580
Case two	$T_{i,i+1}^d(j\omega)$	0.204	0.435	0.528
	$DI_{i,i+1}(j\omega)$	0.03	0.04	0.09

For cases one and two, indicators $DI_{i,i+1}(j\omega)$ in substructure A are always comparatively larger while indicators $DI_{i,i+1}(j\omega)$ in substructure B are close to zero. Therefore, the result is that a potential bolt-loosening fault exists in substructure A only in two cases.

Overall, compared with the case setup in Table 1, the results of the existing approach show that it can detect the bolt-loosening faults in case one only and give wrong fault information in case two. The main reason is that this approach is proposed based on the simple MDOF model, and the properties of nonlinear transmissibility functions and sensitivity of fault indicators are affected by the ignored nonlinear boundaries.

5. Conclusions and discussions

To overcome some limitations in existing nonlinear transmissibility function-based approaches like neglect of nonlinear boundaries and requirement of benchmark data, a novel fault evaluation approach is proposed with detailed theoretical analysis and experimental study. Some conclusions and discussions are summarised as follows:

- (1) By considering simple T-type substructures in complex aerospace structures and simulating the effects of nonlinear boundaries and bolt-loosening faults as nonlinear forces, the general equation of motion of T-type substructures is obtained for the dynamic analysis and fault evaluation.

- (2) By exciting complex aerospace structures four times with different excitation magnitudes, the novel features and sensitive fault indicator of each T-type substructure can be obtained, which does not require reference data and utilises dynamic data of the substructure to be evaluated only.
- (3) Following the procedures, some tests on a bolted structure are implemented to verify the availability of the novel approach. Moreover, comparative results with one existing approach demonstrate that this new approach can give more reliable fault information in structures even with nonlinear boundaries.

The main feature of this novel approach is that it does not need reference features and deal with structures which even have nonlinear boundaries. In future study, an improved approach which has the ability to identify the severity of faults and residual life of damaged structures should be considered to take full advantages of nonlinear transmissibility functions and the T-type model. Moreover, application and extension of this approach to other more complex aerospace structures with bolt-loosening faults such as rotors and stators should be studied as well.

Acknowledgements

This work is supported by a start-up fund of City University of Hong Kong (No. 9380140), fundamental research funds for the central universities (No. 3102020OQD705), and China Scholarship Council (No. 202306290109).

Notes on contributors



Dr Quankun Li received his B.Eng. degree from Nanjing University of Aeronautics and Astronautics, the People's Republic of China, in 2011, M.Eng. degree in Propulsion Theory and Engineering of Aeronautics and Astronautics from Northwestern Polytechnical University, the People's Republic of China, in 2014, and Ph.D. degree in Mechanical Engineering from The Hong Kong Polytechnic University, the People's Republic of China, in 2020, respectively. Dr Li is now an Associate Professor with the School of Power and Energy, Northwestern Polytechnical University. His current research topic is the Dynamic Analysis, Vibration Control and Fault Diagnosis of aerospace structures. Dr Li currently serves as Guest Associate Editor on Vibration Systems of Frontiers in *Mechanical Engineering*. He was Topic Editor of a special issue on 'Rising Stars in Vibration Systems 2022' published in Frontiers in *Mechanical Engineering*.



Prof Xingjian Jing received his B.S. degree from Zhejiang University, the People's Republic of China, in 1998, and M.S. degree and Ph.D. degree in Robotics from Shenyang Institute of Automation, Chinese Academy of Sciences, the People's Republic of China, in 2001 and 2005 respectively. Thereafter, he achieved

a Ph.D. degree in nonlinear systems and signal processing from the University of Sheffield, U.K., in 2008. He is now a Full Professor with the Department of Mechanical Engineering, City University of Hong Kong. His current research interests are generally related to Nonlinear Dynamics, Vibration, and Control focusing on theory and methods for employing nonlinear benefits in engineering, including nonlinear frequency domain methods, nonlinear system identification or signal processing, vibration control, robust control, sensor technology, energy harvesting, nonlinear fault diagnosis or information processing, bio-inspired systems and methods, bio-inspired robotics and control, etc. Prof Jing is the recipient of a series of academic and professional awards including 2016 IEEE SMC Andrew P. Sage Best Transactions Paper Award, 2017 TechConnect World Innovation Award in the U.S, 2017 EASD Senior Research Prize in Europe and 2017 First Prize of the HK Construction Industry Council Innovation Award. He has published more than 120 refereed papers and obtained about 15 patents filed in the People's Republic of China and the U.S. Prof Jing currently serves as Associate Editor of *IEEE Transactions on Systems Man Cybernetics-Systems*, Associate Editor of *IEEE Transactions on Industrial Electronics*, Specialty Chief Editor on *Vibration Systems of Frontiers in Mechanical Engineering*, and Associate Editor of *Mechanical Systems and Signal Processing*. He was Technical Editor of *IEEE/ASME Transactions on Mechatronics* during 2015-2020, and Lead Editor of special issues on 'Exploring nonlinear benefits in engineering' published in *Mechanical Systems and Signal Processing* in 2019 & 2022 respectively. He is also a senior IEEE Member.

References

- [1] Balageas D, Fritzen C, and Güemes A (2010). *Structural health monitoring*. London: ISTE Ltd, pp. 15-18.
- [2] Bickford J (2008). *Introduction to the design and behavior of bolted joints*. Boca Raton: Chemical Rubber Company (CRC) Press, pp. 293-297.
- [3] Bickford J and Nassar S (1998). *Handbook of bolts and bolted joints*. New York: M. Dekker, pp. 757-759.
- [4] B&K.com. (2023a). *Modal exciter 4824*. [online]. Available at: <<https://www.bksv.com/en/instruments/vibration-testing-equipment/modal-exciter/modal-exciter-4824>>. [Accessed on 23 February 2023].
- [5] B&K.com. (2023b). *B&K Vibro accelerometer ASA-20*. [online]. Available at: <ATEX approved ASA-020 Acceleration Sensor - Brüel & Kjær (bkvibro.com)>. [Accessed on 23 February 2023].
- [6] Brown RL and Adams DE (2003). Equilibrium point damage prognosis models for structural health monitoring. *Journal of Sound and Vibration*, 262(3), pp. 591-611.
- [7] Cheng CM, Peng ZK, Dong XJ, Zhang WM and Meng G (2014). Locating non-linear components in two dimensional periodic structures based on NOFRFs. *International Journal of Non-Linear Mechanics*, 67, pp. 198-208.
- [8] Cheng L and Cigada A (2020). An analytical perspective about structural damage identification based on transmissibility function. *Structural Health Monitoring*, 19(1), pp. 142-155.
- [9] Ewins D (2000). *Modal testing: theory, practice and application (mechanical engineering research studies: engineering dynamics series)*. Research studies Pre, 2nd ed., ISBN-13, 978-0863802188.
- [10] Huang J, Liu J, Gong H and Deng X (2022). A comprehensive review of loosening detection methods for threaded fasteners. *Mechanical Systems and Signal Processing*, 168, pp. 108652.
- [11] Jing XJ and Li QK (2016). A nonlinear decomposition and regulation method for nonlinearity characterization. *Nonlinear Dynamics*, 83, pp. 1355-1377.
- [12] Johnson TJ and Adams DE (2002). Transmissibility as a differential indicator of structural damage. *Journal of Vibration and Acoustics*, 124(4), pp. 634-641.
- [13] Johnson TJ, Brown RL, Adams DE and Schiefer M (2004). Distributed structural health monitoring with a smart sensor array. *Mechanical Systems and Signal Processing*, 18(3), pp. 555-572.
- [14] Li QK and Jing XJ (2017). A second-order output spectrum approach for fault detection of bolt loosening in a satellite-like structure with a sensor chain. *Nonlinear Dynamics*, 89, pp. 587-606.
- [15] Li QK and Jing XJ (2020a). Fault diagnosis of bolt loosening in structures with a novel second-order output spectrum-based method. *Structural Health Monitoring*, 19(1), pp. 123-141.
- [16] Li QK and Jing XJ (2020b). A systematic second-order output spectrum-based method for fault diagnosis with a local tuning approach. *Journal of Sound and Vibration*, 475, pp. 115283.
- [17] Li QK, Liao MF and Jing XJ (2021). Transmissibility function-based fault diagnosis methods for beam-like engineering structures: a review of theory and properties. *Nonlinear Dynamics*, pp. 1-33.
- [18] Li QK, Wang R, Liao M and Jing XJ (2022). A novel frequency domain feature-based approach for diagnosis of failure faults in complex structures with interconnected joints. *Mechanical Systems and Signal Processing*, 173, pp. 109064.

- [19] Li XZ, Dong XJ, Peng ZK, Zhang WM and Meng G (2017). Local variation detection in MDOF system using wavelet-based transmissibility and its application in cracked beam. *Journal of Vibration and control*, 23(14), pp. 2307-2327.
- [20] Li XZ, Peng ZK, Dong XJ, Zhang WM and Meng G (2015). A new transmissibility-based indicator of local variation in structure and its application for damage detection. *Shock and Vibration*, 2015, pp. 1-12.
- [21] Liu L, Thomas JP, Dowell EH, Attar P and Hall KC (2006). A comparison of classical and high dimensional harmonic balance approaches for a Duffing oscillator. *Journal of Computational Physics*, 215(1), pp. 298-320.
- [22] Miao R, Shen, R, Zhang S and Xue S (2020). A review of bolt tightening force measurement and loosening detection. *Sensors*, 20(11), pp. 3165.
- [23] Nikravesh S and Goudarzi M (2017). A review paper on looseness detection methods in bolted structures. *Latin American Journal of Solids and Structures*, 14(12), pp. 2153-2176.
- [24] Peng ZK, Lang ZQ, Chu FL and Meng G (2010). Locating nonlinear components in periodic structures using nonlinear effects. *Structural Health Monitoring*, 9(5), pp. 401-411.
- [25] RIGOL.com. (2023). *Function generator DG4000 Series*. [online]. Available at: <<https://int.rigol.com/products/waveform-generators/dg4000.html>>. [Accessed on 23 February 2023].
- [26] Zhao XY, Lang ZQ, Park G, Farrar CR, Todd MD, Mao Z and Worden K (2014). A new transmissibility analysis method for detection and location of damage via nonlinear features in MDOF structural systems. *IEEE/ASME transactions on mechatronics*, 20(4), pp. 1933-1947.
- [27] Zhou YL, Figueiredo E, Maia N and Perera R (2015). Damage detection and quantification using transmissibility coherence analysis. *Shock and Vibration*, 2015, pp. 1-14.